JOURNAL OF SOLID STATE CHEMISTRY 13, 192–200 (1975)

The High Temperature Behavior of In_2O_3

J. H. W. DE WIT

Inorganic Chemistry Department, University of Utrecht, Croesestraat 77A, Utrecht, The Netherlands

Received April 25, 1974

The electrical conductivity of In_2O_3 has been measured up to 1400°C in air. The temperature dependence of the conductivity at high temperatures yields an activation energy of 1.5 ± 0.1 eV. This activation energy is interpreted in terms of a nonstoichiometric decomposition of the compound. This interpretation is sustained by thermogravimetric analysis in combination with a gas mass analyser. Hall experiments on quenched samples are not in contradiction with this interpretation.

Introduction

In 1962 Weiher (*1*) measured the electrical conductivity of In_2O_3 single crystals up to 1500°C in air. Above 1100°C the conductivity of various crystals has the same value with an activation energy of 1.55 eV. We did find the same temperature dependence in the high temperature region for polycrystalline material in air. This high temperature region can be extended to lower temperatures by doping with divalent cations like Mg^{2+} and Ca^{2+}. This was also found by Weiher (*1*) for a Zn-doped crystal. It has been shown that the electrical behavior of In_2O_3 from room temperature to 800°C is influenced by impurities and especially for the polycrystalline samples by oxygen adsorption. Above 800°C these factors are of no importance because they are overshadowed by "intrinsic" properties. Weiher suggested two different mechanisms to explain the huge increase in conductivity above 1100°C. First he considered band to band transitions, and second dissociation of the compound. At first sight both mechanisms seem possible. However, the oxygen pressure dependence of the conductivity in this intrinsic region (*3*, *4*) is a strong indication for the dissociation mechanism. In this paper evidence is presented for this mechanism.

Experimental

The preparation of the materials has been described elsewhere (*3*). The electrical conductivity was measured in a spring loaded furnace, in air up to 1400°C. The conductivity bridge arrangement has also been described before (*3*).

The thermogravimetric analyses were performed with a Dupont equipment in conjunction with a Cahn electrobalance (model RH). This balance has a sensitivity of 1 μg and a precision of 2 μg.

The measurements were performed in an oxygen or a nitrogen gas stream. The nitrogen gas was passed through a BTS catalyst (BASF) for purification and then passed through a molecular sieve (A_4, BDH). The oxygen gas was dried by passing it through a molecular sieve.

The gas flow was 25 cc min^{-1}, while the heating rate normally was 6°C min^{-1}. The suspension wire and the sample holder consisted of sintered alumina. This material induces stronger electrostatical disturbances than platinum, but platinum was not satisfactory because it has a measurable rate of evaporation at temperatures above 1200°C in the microgram region (*5*). A blank run was performed both in nitrogen and oxygen. The resulting standard

deviation for the weight signal in the average of four measurements was 8 μg for the described systems both for nitrogen and oxygen. The oxygen content of the nitrogen gas coming from the T.G. cell was sometimes followed with a Topatron 8 mass analyser (Leybold Heraeus). This mass analyser was equipped with a pressure regulator, to obtain a constant leakage of the gas from the T.G. cell to the vacuum system of the Topatron. The measurements were performed by monitoring the peak height of the mass 32 signal.

The Hall measurements were performed on quenched polycrystalline tablets. Use was made of a magnet with a magnetic field force of 5000 G. The measurements were performed in air. Electrode contacts were provided by means of a platinum paint of Degussa.

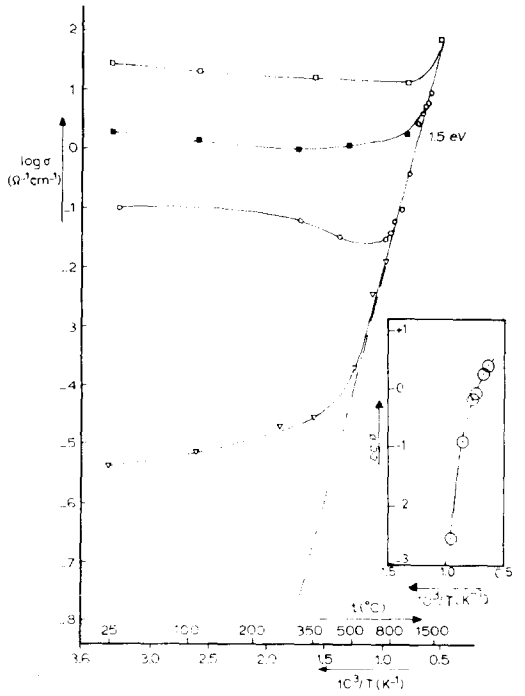

FIG. 1. The electrical conductivity of two polycrystalline In_2O_3 samples in comparison with the single crystalline samples of Weiher (*1*), as a function of temperature in air. —■—■—■—: Single crystal Weiher, doped with Zn; —□—□—□—: single crystal Weiher, undoped; —○—○—○—: polycrystalline sample, undoped; —▽—▽—▽—: polycrystalline sample doped with Ca. FIG. 1a (inset). The electrical conductivity of six Ca doped flux grown crystals as a function of the annealing temperature after quenching to room temperature. The Ca concentration is the same for all six samples.

Results

Figure 1 shows the temperature dependence of the electrical conductivity of two different polycrystalline samples in comparison with the single-crystalline samples of Weiher in air. From this figure it follows that the high temperature region with an activation energy of 1.5 ± 0.1 eV is extended to lower temperatures by doping with Ca or Zn.

Figure 1a (inset) shows the conductivity of six Ca-doped flux-grown crystals as a function of the annealing temperature after quenching to room temperature. The Ca concentration is equal for all six crystals. The conductivity values fit reasonably well to the curve of Fig. 1. This indicates that the temperature dependence of the mobility can be neglected against the carrier concentration dependence on the temperature.

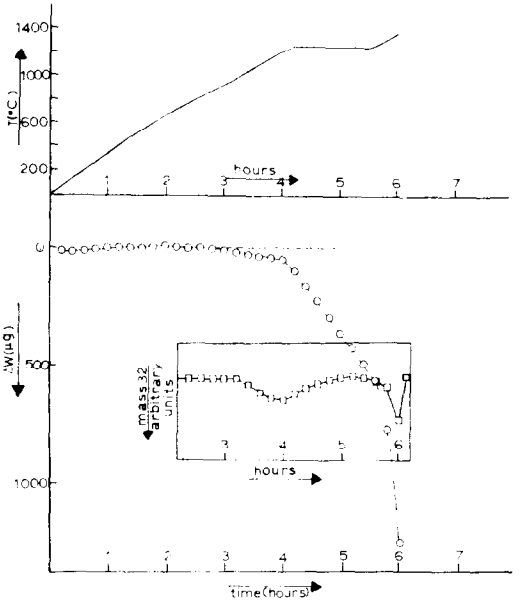

FIG. 2. The weight signal of a 250 mg polycrystalline sample as a function of temperature in a flow of nitrogen. The O_2^{32} mass signal in the evolving gas has been pictured in arbitrary units.

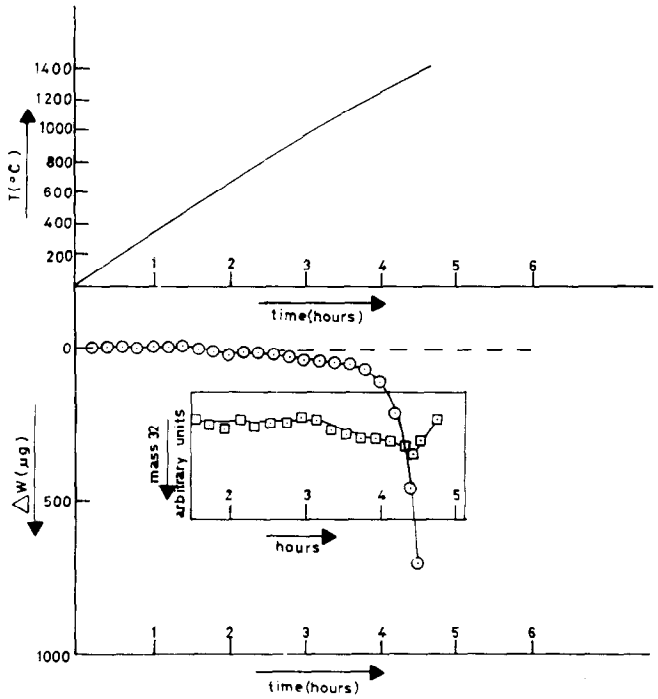

FIG. 3. The weight signal of the same 250 mg sample as used in Fig. 2 is shown again as a function of temperature. This time no isothermal period was recorded. The measurement was performed after an oxygen pretreatment at 900°C.

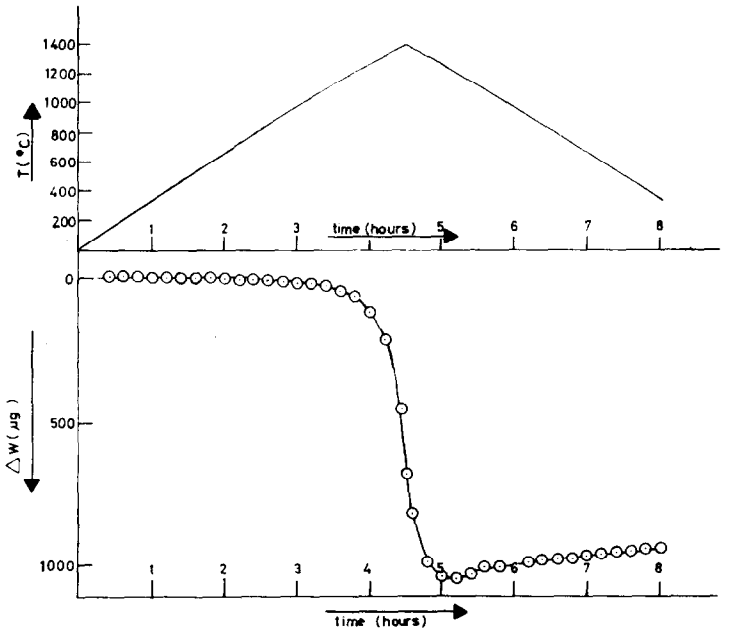

FIG. 4. The result of a T.G. measurement on the same sample. Here the cooling down period was recorded as well.

In Fig. 2 the weight signal of a 250 mg polycrystalline sample as a function of the temperature in a flow of nitrogen is shown. In the same figure the O_2^{32} mass signal in the evolving gas has been plotted. At 900°C the sample starts losing weight, whereas a sudden increase in the reaction rate can be observed at 1200°C. At 1260°C the measurement is continued isothermally, showing a linear weight loss as a function of time. When warming up again a large increase in the reaction rate is observed, resulting in a total weight loss of 1.2 mg after 6 hr.

The O_2^{32} mass signal shows two peaks. The first can be observed at 1200°C, while the second is observed at 1390°C. A single crystalline sample showed the same behavior.

Figure 3 shows the weight signal of the same polycrystalline sample as a function of temperature in nitrogen, after an air pretreatment at 900°C. This time no isothermal period was recorded. Also here the O_2^{32} mass signal has been pictured now showing only one peak at maximum temperature.

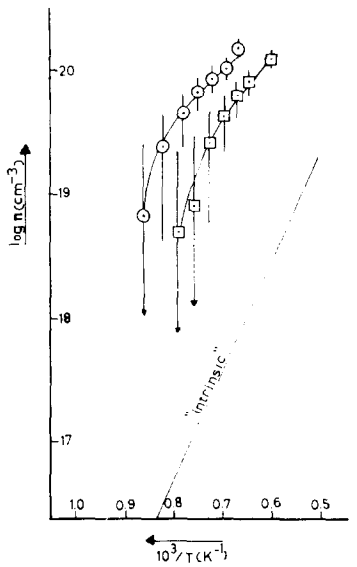

FIG. 5. The electron concentration as a function of temperature, deducted from T.G. measurements. —⊙—⊙—⊙—: The average of four measurements in nitrogen on a single crystal; —□—□—□—: The average of four measurements in oxygen on the same crystal. The true intrinsic electron concentration has been pictured for comparison.

Figure 4 shows the result of a T.G. measurement in nitrogen on the same sample. Now the weight signal was also recorded when cooling the material. A total weight loss of the sample of 1050 μg was observed after heating to 1400°C. Only 110 μg was taken up again after cooling to room temperature.

Figure 5 shows the electron concentration as a function of the reciprocal temperature. This electron concentration was calculated from several T.G. measurements on one crystalline sample. For every missing oxygen atom two electrons were assumed to be added to the conductivity band. The measuring points in Fig. 5 are the average of four measurements both for the oxygen and for the nitrogen measurements.

Discussion

The high temperature region in the $\log\sigma$ vs $1/T$ plot (Fig. 1) shows an activation energy of 1.5 ± 0.1 eV. Upon doping, the material with Ca or Zn the conductivity in the low temperature region is lowered. As a result of this, the onset of the high temperature region is at a lower temperature. We will not discuss the incorporation mechanisms of the cations because it is irrelevant to the purpose of this paper (*2*). The electrical conductivity can be described by:

$$\sigma_t = \sigma_e + \sigma_i = n e b_n + p e b_p + \sigma_i, \qquad (1)$$

where the subscripts t, e and i refer to total, electronic and ionic, n and p denote, respectively, the electron and the hole concentration, e denotes the electronic charge and b denotes the mobility.

The room temperature Hall coefficient for samples quenched from temperatures between 800 and 1400°C was always negative. The oxygen pressure dependence of the conductivity between 800 and 1000°C can be given by (*2*, *3*)

$$\sigma \approx p_{O_2}{}^{1/n}, \qquad (2)$$

where n denotes a digit. These two properties strongly suggest a predominantly n-type semiconductivity, as was also found for the low-temperature region (*3*).

In literature a p-type behavior of In_2O_3 has

never been reported. We will therefore neglect the second term in Eq. (1). The third term represents a possible ionic contribution to the conductivity. Because of the distinct oxygen pressure dependence of the conductivity it is improbable that this term will be of great importance. In principle at least two kinds of ionic defects could contribute to this term: oxygen vacancies and indium interstitials. The measurements of Rosenberg (*6*, *7*) of the oxidation rate of In metal suggest the movement of $In_i^{\cdots}$ defects. However, when extrapolating from his temperature range (308–407°C) to our high temperature region is allowed, we only reach values of about 0.1% of the observed conductivity.

This is sustained by electrolysis experiments we performed on In_2O_3 according to Tubandt.

Through three sintered tablets of In_2O_3 fitted between two platinum electrodes, a stabilized dc current of 1 A was led during several weeks, at a temperature of 900°C, in air. From the weight changes of the anodic and the kathodic tablets it was concluded that an $In_i^{\cdots}$ transport contribution was smaller than 0.1% of the total conductivity. The movement of oxygen vacancies cannot be measured in such a single way. So until now we cannot exclude the possibility of a small ionic contribution by some kind of mobile oxygen defect. However, because of reasons mentioned above, we will neglect the ionic term in Eq. (1) of this paper.

Equation (1) then reduces to $\sigma_t = \sigma_e = n\,e\,b_n$. (3)

From our measurements in air it follows (see Fig. 1) that:

$$\sigma = \sigma_o \exp\{-(1.5 \pm 0.1)\,\mathrm{eV}/kT\}. \quad (4)$$

We will first consider the possibility of true intrinsic behavior, although the oxygen pressure dependence does not suggest this mechanism.

For true intrinsic behavior statistical mechanics lead to Eq. (5):

$$n_i = \frac{2(2\pi mkT)^{3/2}}{h^3} \cdot \left(\frac{m_n^*\, m_p^*}{m^2}\right)^{3/4} \times \exp - \{Eg^0/2kT - \beta/2k\} \quad (5)$$

for the case $E_g{}^T = E_g{}^0 - \beta T$ (eV).

n_i denotes the intrinsic electron concentration, m the free electron mass, k the Boltzmann constant, h Planck's constant, T the absolute temperature, m_n^* and m_p^*, the effective mass of the electrons and the holes, respectively, E_g° the band gap at absolute zero and β the temperature coefficient of the band gap.

Equation (5) can be written as:

$$n_i = C_1\, T^{3/2} \exp - (E_g{}^0/2kT - \beta/2k), \quad (5)$$

where C_1 denotes a constant.

The mobility can be represented by

$$b_n = C_2 \exp(-\Delta H_m/kT), \quad (6)$$

where ΔH_m denotes the activation energy for the motion of the electrons.

Furthermore, the following approximation can be used in the temperature range of 800–1400°C:

$$T^{+3/2} = C_3 \exp(-\alpha/kT). \quad (7)$$

A combination of Eq. (7) and Eq. (5) gives:

$$n_i = C_4 \exp -\{E_g{}^0/2kT - \beta/2k + \alpha/kT\}. \quad (8)$$

This equation can be simplified to:

$$n_i = C_5 \exp -\{E_g{}^0/2kT + \alpha/kT\}. \quad (9)$$

Then a combination of Eqs. (3), (6), and (9) gives:

$$\sigma_e = C_6 \exp -\{E_g{}^0/2kT + \alpha/kT + \Delta H_m/kT\}, \quad (10)$$

where $C_6 = e\,C_5C_2$.

From a combination of Eq. (4) and Eq. (10) follows, after differentiating against reciprocal temperature:

$$E_g{}^0 + 2(\Delta H_m + \alpha) = 3.0 \pm 0.2\,\mathrm{eV}.$$

Now for the case that $\Delta H_m = -\alpha$ follows that

$$E_g{}^0 = 3.0 \pm 0.2\,\mathrm{eV}.$$

The band gap of In_2O_3 at room temperature can be represented by $E_g^{297} = 2.8$ eV with a temperature coefficient of -1.10^{-3} eV deg^{-1} (*8*, *9*).

The value of 3 eV for $E_g{}^0$ therefore seems to fit for the case that $\Delta Hm = -\alpha$. This means recalling Eqs. (6) and (7) that $b_n \approx T^{-3/2}$, which is not in contradiction with previously published data concerning the temperature de-

pendence of the electron mobility in In_2O_3(*3*).

However, not only the activation energy should fit to the experimental data. At the same time the electron concentration should reach the high values as represented in Fig. 5. These values were obtained from T. G. measurements. Hall measurements on quenched samples in air yield electron concentrations for this temperature region between 10^{19} and 10^{20} electrons cm^{-3}, in good agreement with the values from the T.G. measurements.

To control whether the information on quenched material can be compared with the dynamic measurements some conductivity measurements were performed with quenched crystals as has been represented in Fig. 1a. This curve shows a good agreement with the $\log\sigma$ vs $1/T$ plot in Fig. 1. When as a first approximation the factor

$$\left(\frac{m_n^* \cdot m_p^*}{m^2}\right)^{3/4} \text{ in Eq. (5) is taken unity,}$$

Eq. (5) leads to electron concentrations of about a factor 100–1000 smaller than the values in Fig. 5. According to Weiher (*1*) and Vainshtein (*10*) the effective mass of electrons in In_2O_3 is $(0.5 \pm 0.1)m_0$. When this value is used in Eq. (5) improbably high values of m_p^* would result from a fit of Eq. (5) to the electron concentration in Fig. 5. Therefore we reject band to band transitions as an explanation for the conduction in the high temperature region as was already suggested by the oxygen pressure dependence of the conductivity. The dissociation of In_2O_3 can be described (*3*) by:

$$2\,In_{In}^{x} + 3O_O^{x} \leftrightarrows 3\,V_O^{\cdot\cdot} + 2\,In_{In}^{x} + 6e' + 3/2\,O_2, \quad (11)$$

or

$$2\,In_{In}^{x} + 3O_O^{x} \leftrightarrows 2\,In_i^{\cdot\cdot\cdot} + 6e' + 3/2\,O_2. \quad (12)$$

Equation (11) holds for the case that the doubly ionized oxygen vacancies are the majority defects, while Eq. (12) is valid when interstitial triply ionized indium atoms are the majority defects.

The oxygen pressure dependence of the equilibrium described by Eq. (11) or Eq. (12) at 800°C has been described before (*3*). Within the experimental error no difference between Eq. (11) and Eq. (12) could be observed. According to either one of the two equilibria it may be expected that when warming up a crystal of In_2O_3 it loses some oxygen resulting in a nonstoichiometric material as has been observed for other oxides like, e.g., CdO (*13*). Above a certain temperature also sublimation of the compound may be expected.

According to Fig. 2 the weight loss starts at a temperature of 900°C in a flow of nitrogen. At 1200°C a sudden increase in the reaction rate is observed. We believe that this sudden increase in weight loss indicates the start of sublimation of In_2O_3, whereas the weight loss between 900 and 1200°C is determined by Eq. (11) or Eq. (12). The gaseous species over In_2O_3 at temperatures above 600°C are predominantly $In_2O(g)$, and $O_2(g)$ as has been shown mass spectrometrically by Burns et al. (*12*). In the gas phase they did not observe any molecules of $In_2O_3(g)$. This was confirmed by Shschukarev et al. (*15*) although in contradiction with a former publication by these authors (*14*). Chatterji and Vest (*11*) did confirm these observations after a theoretical evaluation of various thermodynamic data of the In–O system. Van Dillen et al. (*16*) gave some more precise data on this system. According to these literature references the sublimation of In_2O_3 is dissociative and can be given by:

$$In_2O_{3(s)} \rightarrow In_2O_{(g)} + O_{2(g)}. \quad (13)$$

The relation between p_{In_2O}, p_{O_2} and T for the gas mixture over In_2O_3 can be given by (*16*).

$$\log p_{In_2O} = -42{,}189/T + 17.7 - \log p_{O_2}. \quad (14)$$

At a heating rate of 6°C/min and a gas flow of 25 cc/min an average ΔW signal of 1 μg/min was observed for the temperature region between 900 and 1200°C (see Fig. 2). Now, when we accept that all the gas is carried off immediately by the flow and that the gas production is not limited by diffusion we can use the partial pressure as found from Eq. (14) to determine the ΔW/time signal as a result from the sublimation according to reaction (*13*). The results of these arithmetics using

$$p_{In_2O} = \frac{dn_{In_2O}/dt}{(dn_{N_2}/dt + dn_{In_2O}/dt)} \cdot p_{tot}, \quad (15)$$

TABLE I

THE PARTIAL PRESSURE OF In_2O AND THE ΔW/TIME SIGNAL AS A FUNCTION OF THE TEMPERATURE

Temperature (°C)	I p_{In_2O} (atm) (according to Eq. (13)	II p_{In_2O} (atm) ($p_{O_2} = 10^{-5}$)	III p_{In_2O} (atm) ($p_{O_2} = 10^{-4}$)	ΔW/time (μg/min) I	II	III
900	7.4×10^{-10}	5.6×10^{-14}	5.6×10^{-14}	2.0×10^{-4}	1.6×10^{-8}	1.6×10^{-9}
1000	2.5×10^{-8}	4.0×10^{-11}	4.0×10^{-12}	6.9×10^{-3}	1.1×10^{-5}	1.1×10^{-6}
1100	2.8×10^{-7}	7.9×10^{-9}	7.9×10^{-10}	7.7×10^{-2}	2.2×10^{-3}	2.4×10^{-4}
1200	3.4×10^{-6}	1.2×10^{-6}	1.2×10^{-7}	9.3×10^{-1}	3.2×10^{-1}	3.2×10^{-2}
1300	2.8×10^{-5}	2.8×10^{-5}	7.6×10^{-6}	7.6	7.6	2.1

where dn_{In_2O}/dt is the number of moles $In_2O(g)$ that vaporizes per second, dn_{N_2}/dt is the flow rate in moles per second of the nitrogen carrier gas, and p_{tot} is the total pressure in the system, can be found in Table I.

It can be seen that only at temperatures of 1200°C or more reaction (*13*) can be responsible for the ΔW signal even for the case that the partial pressure of the oxygen gas in the carrier nitrogen gas is smaller than 10^{-5} atm which is not probable. The estimated oxygen partial pressure lies between 10^{-5} and 10^{-4} atm. Therefore, we conclude that no sublimation according to Eq. (13) can account for the weight loss under 1200°C. whereas this sublimation can be responsible for the weight loss above 1200°C. This explains the sudden increase of the ΔW/time signal at 1200°C. Furthermore, we believe that the weight loss under 1200°C should be attributed to the dissociation of In_2O_3 according to Eq. (11) or Eq. (12). This mechanism is sustained by the O_2^{32} mass signal. The increase of this signal up to 1200°C (see Fig. 2) results from the evolving O_2 according to Eq. (11) or Eq. (12). The decrease of the O_2^{32} signal during the isothermal period at 1260°C can be explained as follows.

During the warming up period the oxygen gas pressure resulting from Eq. (12) or Eq. (11) was larger than the partial oxygen pressure in the nitrogen carrier gas; since no equilibrium situation could be reached this situation persisted till the isothermal period. Here a stable situation is reached when the partial oxygen pressure levels up with the original partial oxygen pressure in the nitrogen gas which means at the same time that the In_2O_3 gets slightly more defect in this dynamic system than in equilibrium with its own atmosphere at the same temperature. The Topatron (O_2^{32}) signal returns to its original level (see Fig. 2) .At the same time the $In_2O(g)$ vapor, which cannot exist below 600°C, is cooled below this temperature before leaving the thermobalance. This vapor then disproportionates according to:

$$3\,In_2O_{(g)} \leftrightarrows In_2O_{3_{(s)}} + 4\,In_{(l,g)}. \qquad (16)$$

The increasing O_2^{32} signal, when warming up again, also results from Eq. (11) or Eq. (12), because the $In_{(l,g)}$ produced according to Eq. (16) will act as a getter for the equivalent amount of oxygen produced according to Eq. (13):

$$4\,In + 3\,O_2 \rightarrow 2\,In_2O_3. \qquad (17)$$

When no isothermal period is introduced, no minimum in the O_2^{32} mass signal is observed as can be seen in Fig. 3, which sustains our theory. Furthermore, when the weight signal is also observed (see Fig. 4) during cooling only below 1200°C a small weight increase can be observed. Between 1400 and 1200°C the sublimation rate gets smaller until at 1200°C it is overshadowed by the oxygen take up according to Eq. (11) or (12). Between 1200 and 900°C 55 μg is taken up by a sample of 250 mg; this is the same amount which was lost during the heating period from 900–1200°C.

Based on this nonstoichiometric decomposition model, Fig. 5 shows the logarithmus of the electron concentration as a function of recip-

rocal temperature for the case that every missing oxygen atom contributes two electrons to the conductivity band. The upper curve is valid for a nitrogen atmosphere and the lower for an oxygen atmosphere. These curves are obtained by taking the average of four thermogravimetric measurements with the same sample both for nitrogen and for oxygen. For the 250 mg crystalline sample used a ΔW signal of 7.5 μg represents an amount of oxygen equivalent to 2×10^{19} electrons cm^{-3}. The error represented in Fig. 5 is the standard deviation in the average of four measurements. For the lower concentrations the lower limit has only been indicated qualitatively by arrows. The good agreement between these values and the Hall electron concentrations in quenched samples, as mentioned above, does sustain our model for the high temperature behavior of In_2O_3.

The Carrier Concentration

From Eq. (11) and the electroneutrality condition $2[V_O^{\cdot\cdot}] = n$ follows with a simple mass action formalism:

$$n = \{8 \cdot K_{ox} \cdot p_{O_2}^{-3/2}\}^{1/9}, \tag{18}$$

where

$$K_{ox} = [V_O^{\cdot\cdot}]^3 \cdot n^6 \cdot p_{O_2}^{+3/2}$$

For the free energy of reaction (11) can be written

$$\Delta G_{ox} = -kT \ln K_{ox} \tag{19}$$

where

$$\Delta G_{ox} = \Delta H_{ox} - T\Delta S_{ox}. \tag{20}$$

From Eq. (18) and Eq. (19) follows:

$$n = 1.26 p_{O_2}^{-1/6} \exp(-\Delta G_{ox}/9kT). \tag{21}$$

Introducing Eq. (21) and Eq. (20) into Eq. (3) gives:

$$\sigma_e = (1.26)\, e\, b_n\, p_{O_2}^{-1/6} \times \exp(-\Delta H_{ox}/9kT + \Delta S_{ox}/9k). \tag{22}$$

Introducing Eq. (6) into Eq. (22) gives:

$$\sigma_e = (1.26)\, e\, C_2 p_{O_2}^{-1/6} \times \exp(-\Delta H_{ox}/9kT + \Delta S_{ox}/9k - \Delta H_m/kT). \tag{23}$$

Recalling Eq. (7):

$$T^{+3/2} = C_3 \exp(-\alpha/kT)$$

and accepting that $H_m = -\alpha$ we can neglect ΔH_m against the carrier concentration dependence on T for this high temperature region. A combination of Eq. (23) with Eq. (4) gives then:

$$\Delta H_{ox} = 9(1.5 \pm 0.1)\text{eV} = (13.5 \pm 0.9)\text{eV}. \tag{24}$$

Using Eq. (12) instead of Eq. (11) gives:

$$\Delta H'_{ox} = 8(1.5 \pm 0.1)\,\text{eV} = (12.0 \pm 0.8)\,\text{eV}. \tag{25}$$

Because of the inaccuracy of Fig. 5 no quantitative interpretation of the slope of this curve can be given. This kind of direct interpretation of a log n vs $1/T$ plot should await more detailed Hall measurements.

Conclusions

The high temperature electrical behavior of In_2O_3 is not determined by interband transitions but by a nonstoichiometric dissociation according to

$$2\,In_{In}^{x} + 3\,O_O^{x} \rightarrow 3\,V_O^{\cdot\cdot} + 6e' + 3/2\,O_2 + 2\,In_{In}^{x}, \tag{11}$$

or

$$2\,In_{In}^{x} + 3\,O_O^{x} \rightarrow 2\,In_i^{\cdot\cdot\cdot} + 6e' + 3/2\,O_2. \tag{12}$$

From the slope of the $\log\sigma$ vs $1/T$ plot a value for the ΔH_{ox} of these reactions can be deduced:

$\Delta H_{ox} = (13.5 \pm 0.9)$ eV for equilibrium 11 and $\Delta H'_{ox} = (12.0 \pm 0.8)$ eV for equilibrium 12.

Only above 1200°C, and in a flow of nitrogen with $p_{O_2} = 10^{-5}$ until 10^{-4} atm sublimation of In_2O_3 takes place at a measurable rate (See Table I).

This sublimation is dissociative and can be represented by:

$$In_2O_{3(s)} \rightarrow In_2O_{(g)} + O_{2(g)}. \tag{13}$$

Acknowledgments

The present investigations have been carried out under the auspices of the Netherlands Foundation for Chemical Research (SON) and with financial aid from

the Netherlands Organization for the Advancement of Pure Research (ZWO). The author is most grateful for the many T.G. measurements Mr. A. Broersma performed for him.

He is also indebted to Prof. Dr. W. van Gool and Dr. J. Schoonman for valuable criticism during the preparation of the manuscript.

References

1. R. L. Weiher, *J. Appl. Phys.* **33**, 9, 2834 (1962).
2. J. H. W. de Wit, H. van Unen, and M. Lahey to be published.
3. J. H. W. de Wit, *J. Solid State Chem. 8*, 142 (1973).
4. G. Rupprecht, *Z. für Physik* **139**, 504 (1954).
5. A. H. Verdonk, thesis, University of Utrecht (1970).
6. A. J. Rosenberg, *J. Phys. Chem.* **64**, 1143 (1960).
7. A. J. Rosenberg and M. C. Lavine, *J. Phys. Chem.* **64**, 1135 (1960).
8. R. L. Weiher and B. G. Dick, *J. Appl. Phys.* **35**, 12, 3511 (1964).
9. R. L. Weiher and R. P. Ley, *J. Appl. Phys.* **27**, 1, 299 (1966).
10. V. M. Vainshtein and V. I. Fistul, *Sov. Phys. Semicond.* **1**, 1, 104 (1967).
11. D. Chatterji and R. W. Vest, *J. Amer. Ceram. Soc.* **55**, 11, 575 (1972).
12. R. P. Burns, G. DeMaria, J. Drowart, and M. G. Ingraham, *J. Chem. Phys*, **38**, 1035 (1963).
13. F. P. Koffyberg, *J. Solid State Chem.* **2**, 176 (1970).
14. S. A. Shchukarev, G. A. Semenov, and I. A. Rat'kovskii, *Zhur. Prikl. Khim.* **35**, 1454 (1962).
15. S. A. Shchukarev, G. A. Semenov, and I. A. Rat'kovskii, *Russ. J. Inorg. Chem.* **14**, 1 (1969).
16. A. J. van Dillen, thesis, University of Utrecht, to be published.